Learning 3D Texture-Aware Representations for Parsing Diverse Human Clothing and Body Parts

Kiran Chhatre^{1,2}, Christopher Peters¹, Srikrishna Karanam²

¹KTH Royal Institute of Technology ²Adobe Research https://s-pectrum.github.io



Figure 1: **Human-alphabet parsing in the wild.** Internet-video frames show people forming the letters of our model name, Spectrum, while the model segments diverse clothing and body part, handling unseen items such as *sarees*, across complex poses and styles. Prompts (shown in teal) also include the extended body-part set (EBP; see Sec. Experiments).

Abstract

Existing methods for human parsing into body parts and clothing often use fixed mask categories with broad labels that obscure fine-grained clothing types. Recent openvocabulary segmentation approaches leverage pretrained text-to-image (T2I) diffusion model features for strong zeroshot transfer, but typically group entire humans into a single person category, failing to distinguish diverse clothing or detailed body parts. To address this, we propose Spectrum, a unified network for part-level pixel parsing (body parts and clothing) and instance-level grouping. While diffusionbased open-vocabulary models generalize well across tasks, their internal representations are not specialized for detailed human parsing. We observe that, unlike diffusion models with broad representations, image-driven 3D texture generators maintain faithful correspondence to input images, enabling stronger representations for parsing diverse clothing and body parts. Spectrum introduces a novel repurposing of an Image-to-Texture (I2Tx) diffusion model—obtained by fine-tuning a T2I model on 3D human texture maps—for improved alignment with body parts and clothing. From an input image, we extract human-part internal features via the I2Tx diffusion model and generate semantically valid masks aligned to diverse clothing categories through prompt-guided grounding. Once trained, Spectrum produces semantic segmentation maps for every visible body part and clothing category, ignoring standalone garments or irrelevant objects, for any number of humans in the scene. We conduct extensive cross-dataset experiments—separately assessing body parts, clothing parts, unseen clothing categories, and full-body masks—and demonstrate that Spectrum consistently outperforms baseline methods in prompt-based segmentation.

Introduction

Human parsing (Xia et al. 2017, 2016; Luo et al. 2018; Gong et al. 2018a; Li et al. 2022d; Gong et al. 2017; Fang et al. 2018) decomposes a human image into distinct parts such as clothing items and body regions. This task provides rich descriptions for human-centric visual analysis (Lin et al. 2019) and has become increasingly important in applications such as person re-identification (Zheng et al. 2019), behavior analysis (Wang, Wang, and Yuille 2013; Wang et al. 2012), fashion synthesis (Zhu et al. 2017), human-object interaction (Gkioxari, Girshick, and Malik 2015), portrait segmentation (Shen et al. 2017, 2016), pedestrian detection (Zhang et al. 2016; Mao et al. 2017), and video surveillance (Lu et al. 2014; Gan et al. 2016). A detailed understanding of

human body structure and the vast diversity in apparel is critical for advancing fields that analyze human appearance in various contexts, especially in complex scenes like those in fig. 1 (top), where the human alphabet forming our model name, Spectrum, shows individuals wearing a range of formal, casual, and traditional attire.

Existing parsing methods typically rely on fixed, predefined categories. Although these are sufficient for human body parts, they struggle to handle the large variability and complexity of clothing in real world contexts, often producing broad or incorrect labels (e.g., labeling all clothing in the torso as 'upper clothes' (Liu et al. 2022; Li et al. 2017; Gong et al. 2018b; Khirodkar et al. 2024; Liang et al. 2015; Gong et al. 2017)). Clothing fashion evolves rapidly, with new styles emerging while older ones become rare, and accessories (e.g., hats, bags, belts, jewelry), as well as traditional attire (e.g., police uniforms, sarees), add further variation. Although recent high-quality annotated datasets (Li et al. 2024; Rasheed et al. 2024; Schuhmann et al. 2022b) capture this diversity, most current parsing architectures still work with a fixed set of labels, making it difficult to fully accommodate new or unseen clothing categories.

Emerging open-vocabulary approaches leverage diffusion models trained on large-scale text-image datasets, demonstrating strong compositional generalization and semantic control (Rombach et al. 2022; Nichol et al. 2022; Saharia et al. 2022; Esser et al. 2024). However, they fail to distinguish body parts or fine-grained clothing, instead labeling the entire human as a single 'person' mask in datasets such as COCO (Mottaghi et al. 2014a), because their broad representations are not specialized for detailed human parsing. Effective human parsing requires both partlevel segmentation—capturing diverse clothing and distinct body parts—and instance-level grouping (e.g., distinguishing each individual's hands in multi-person scenes). Recent multimodal text and image driven 3D texture generation models show faithful correspondence to input modalities (Tu et al. 2025; Casas and Comino-Trinidad 2023). We observe that these strong 3D texture-based features can significantly enhance segmentation of diverse human clothing and body parts. To address existing limitations in finegrained human parsing, we leverage diffusion models finetuned on high-quality 3D human texture maps from the AT-LAS dataset (Liu et al. 2024), enabling accurate segmentation of diverse clothing categories and body parts.

In Spectrum, we utilize these specialized internal representations that capture body parts and clothing features more effectively than standard diffusion model representations. We leverage the large-scale CosmicManHQ dataset (Li et al. 2024), which contains detailed real-world images with text annotations describing human clothing and body parts, and focus exclusively on parsing on-body clothing, ignoring standalone garments or irrelevant items. Specifically, our model takes an image and a descriptive caption as input and outputs segmentation maps with semantic annotations for every visible body part and clothing category in scenes with any number of humans. To the best of our knowledge, our unified network is the first to offer this capability, which current human parsing and open-vocabulary segmentation

methods lack. We use ground-truth masks for broad bodypart categories and generic garment classes from Cosmic-ManHQ to supervise the model, producing class-agnostic masks aligned with scene-specific prompts—enabling the parsing of both seen and unseen clothing categories. We validate our method through four evaluation setups: FPP (Full-Person Parsing, merging each person into one mask), BHP (Bare Human Parsing, separating each visible body part), CCP (COCO Category Parsing, focusing on human-relevant COCO accessory classes), and COP (Clothing-Only Parsing, isolating each clothing instance). Experiments on CosmicManHQ's test set and cross-dataset scenarios demonstrate our model's effectiveness in handling diverse clothing and body parts more effectively than existing human parsing and open-vocabulary segmentation approaches. As shown in fig. 1 (bottom), the model accurately segments formal (suit, trouser) and casual (shorts, jacket) attire in in-thewild images, including unseen traditional clothing (sarees).

Our key contributions are: (1) We introduce Spectrum, to the best of our knowledge the first human parsing approach that jointly addresses part-level pixel parsing for diverse on-body clothing, body parts, and instance-level part grouping via a unified network. (2) We repurpose an Image-to-Texture (I2Tx) diffusion model—fine-tuned from a T2I backbone on 3D human texture maps—to align internal features with diverse on-body clothing and body parts, enabling precise human parsing. (3) Extensive cross-dataset experiments in four setups (FPP, BHP, CCP, COP) show that Spectrum consistently outperforms existing methods when parsing scenes with any number of humans.

Related Work

Human Parsing

Early methods in human parsing focused on multiscale image features (Chen et al. 2018, 2016; Long, Shelhamer, and Darrell 2015), human pose (Xia et al. 2016; Dong et al. 2014; Ladický, Torr, and Zisserman 2013), or visual cues as weak supervision (Chen, Shrivastava, and Gupta 2014; Dai, He, and Sun 2015). Broadly, human parsing can be divided by the number of human instances in the data and input modality: single-human parsing (e.g., (Gong et al. 2017; Liang et al. 2015; Luo, Wang, and Tang 2013; Dickens and Hamad 2025)), multi-human instance-level parsing (e.g., (Mottaghi et al. 2014b; Liu et al. 2025)), and videobased parsing (e.g., (Zhou et al. 2018; Gupta et al. 2023; Qian et al. 2023; Li et al. 2022c)), although our scope is image-based single- and multi-human parsing. In singlehuman parsing, SST (Yang et al. 2023) unifies label domains to train universal and dedicated parsing networks, CDGNet (Liu et al. 2022) accumulates horizontal/vertical human-part distributions with attention for accurate relationship modeling, SCHP (Li et al. 2022d) addresses annotation noise via self-correction, and SAPIENS (Khirodkar et al. 2024) exploits a ViT-based masked autoencoder pretrained on large-scale human images. In multi-human parsing, RP R-CNN (Yang et al. 2020) introduces a semanticenhanced feature pyramid and parsing re-scoring network, while AIParsing (Zhang et al. 2022) takes a one-stage topdown approach for instance detection and part segmentation. Most previous methods rely on ground-truth image masks with fixed parsing labels, lacking dense annotations of human attributes and real-world complexity (Gong et al. 2017; Liang et al. 2015), thus producing coarse results that cannot handle new categories to align masks categorically. We address this gap by pursuing robust fine-grained parsing for body parts and diverse clothing, incorporating instance-level part grouping in a unified network.

Open-vocabulary Segmentation

Background. Open-domain tasks have gained increasing attention for their ability to handle unseen categories during inference (Zhu and Chen 2024). These include openset recognition (Geng, Huang, and Chen 2021), out-of-distribution detection (Zhang et al. 2024), open-world recognition (Kim et al. 2022a; Bendale and Boult 2015), open-vocabulary learning (Wu et al. 2024), and zero-shot learning (Xian et al. 2019). Large vision–language models (VLMs) trained with image—text contrastive objectives provide strong zero-shot transfer (Radford et al. 2021; Jia et al. 2021), and T2I models further bind region—word correspondences (Ho, Jain, and Abbeel 2020; Rombach et al. 2022). Below, we review open-vocabulary semantic and instance segmentation methods relevant to our work.

Semantic segmentation. Recent open-vocabulary semantic segmentation methods adapt pretrained VLMs or diffusion models to segment novel classes. ODISE (Xu et al. 2023) uses frozen T2I diffusion features and an implicit captioner, while MaskCLIP (Zheng Ding 2023) modifies CLIP's (Radford et al. 2021) final attention layer for stronger local semantic consistency. IFSeg (Yun et al. 2023) processes target categories given only label sets, and GD (Li et al. 2023) aligns T2I model's visual and textual embeddings via a grounding module. OVSeg (Liang et al. 2023) finetunes CLIP with mask-category pairs to overcome domain gaps, and OVAM (Manchón et al. 2024) generates wordspecific attention maps in T2I models without additional training. SED (Xie et al. 2024) applies a hierarchical encoder-decoder for cost-map generation, while SEEM (Zou et al. 2023) employs prompt-based interactive segmentation. OpenSeg (Ghiasi et al. 2022b) randomly drops words during training to prevent overfitting. Broadly, some T2I-based methods synthesize labeled images (Li et al. 2022a; Zhang et al. 2021) or perform image conditioning for mask generation (Amit et al. 2022; Ji et al. 2023; Chen et al. 2023).

Instance segmentation. GGN (Wang et al. 2022) uses pseudo supervision from learned pixel-level affinities, OLN (Kim et al. 2022b) applies classifier-free object localization, and OV-SAM (Yuan et al. 2024) merges CLIP and SAM for open-vocabulary recognition. Despite the successes of open-vocabulary methods, these approaches rarely address fine-grained human body parts or complex clothing categories, often collapsing people into a single *person* mask. We bridge this gap by adapting open-vocabulary segmentation to detailed body-part and clothing parsing for arbitrary humans. To this end, we adopt a fine-tuned T2I model on human textures, yielding specialized representations that enable accurate segmentation of detailed body parts and di-

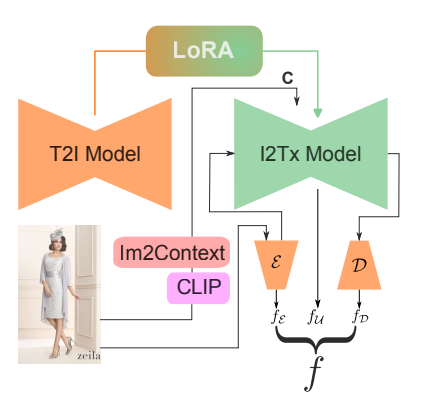


Figure 2: **I2Tx feature extraction.** Base SD weights are merged with 3D-texture LoRA matrices, and a context embedding \mathbf{C} from IM2CONTEXT and CLIP-VISION drives a single forward pass in the I2Tx model. Concatenating encoder, denoiser, and decoder representations yields the texture-aligned feature f for clothing and body-part parsing.

verse clothing.

Method

Overview. We focus on prompt-based human parsing for diverse clothing categories and individual body parts. During training, ground truth masks for 17 generic base categories and dense captions are provided; body part masks are detailed, whereas clothing masks are weakly annotated because the base categories (e.g., *Special Clothings, One-piece Outfits*) are broad and require grounding to learn accurate labels. At test time, clothing may include both seen and unseen classes, and we ensure that the test subset explicitly includes unseen categories for separate evaluation.

Repurposing Image-to-Texture Models

Preliminaries. We leverage strong 3D texture-based features with faithful correspondence to input images to enhance segmentation of diverse clothing and body parts. Consequently, we repurpose diffusion features from Tex-Dreamer (Liu et al. 2024), a dual-conditioned (text/image) 3D texture generator, for 2D human parsing. TexDreamer builds on Stable Diffusion (SD) (Rombach et al. 2022) with LoRA (Hu et al. 2022), trained on 3D human texture maps paired with images and captions from the ATLAS dataset. It conditions on image features from the IM2CONTEXT encoder, whose LoRA weights and pretrained encoder we reuse in our method.

I2Tx feature extraction. As illustrated in fig. 2, our feature-extraction pipeline uses the frozen I2Tx architecture in a single forward pass, omitting iterative denoising. We first merge the base SD weights $W_{\phi_{\text{SD}}} \in \mathbb{R}^{d \times k}$ with Tex-Dreamer's LoRA matrices $B \in \mathbb{R}^{d \times r}$ and $A \in \mathbb{R}^{r \times k}$ (with $r \ll \min(d,k)$), so the adapted projection becomes $W_{\phi_{\text{SD}}} + BA$. An input image x is then encoded by the CLIP-VISION encoder ϕ_{CV} and the IM2CONTEXT encoder ϕ_{I2C} to generate the context embedding ${\bf C}$ and the CLS token.

$$\mathbf{C} = \phi_{\text{I2C}} \left\{ \phi_{\text{CV}}(x) \right\} \tag{1}$$

The encoder $\phi_{\mathcal{E}}$ produces features $f_{\mathcal{E}}$ and a latent code x_e . A noisy latent is sampled with noise schedule $\bar{\alpha}_t = \prod_{k=1}^t \alpha_k$ as (Nichol and Dhariwal 2021; Ho, Jain, and Abbeel 2020).

$$f_{\mathcal{E}}, x_e = \phi_{\mathcal{E}}(x),$$

$$x_t \triangleq \sqrt{\overline{\alpha}_t} x_e + \sqrt{1 - \overline{\alpha}_t} \epsilon, \quad \epsilon \sim \mathcal{N}(0, \mathbf{I}),$$
(2)

The denoiser $\phi_{\rm SD}$ is conditioned on $(x_t, {\bf C}, {\rm CLS})$ to yield f_U , while the decoder $\phi_{\mathcal D}$ processes x_t to obtain $f_{\mathcal D}$. Concatenating the encoder, denoiser, and decoder streams yields a texture-aligned representation f that drives our segmentation head to parse on-body clothing and body parts.

$$f_{U} = \phi_{\text{SD}}(x_{t}, \mathbf{C}, \text{CLS})$$

$$f_{\mathcal{D}} = \phi_{\mathcal{D}}(x_{t})$$

$$f = f_{\mathcal{E}} \parallel f_{U} \parallel f_{\mathcal{D}}$$
(3)

Semantically Grounded Parsing

Parsing head architecture. As shown in fig. 3, a pixel decoder \mathcal{P} (implemented as a feature-pyramid network (Cheng et al. 2022a; Wu et al. 2019; Zhu et al. 2021)) converts the texture representation f into multi-scale, high-resolution per-pixel embeddings. Its final mask feature $f_{\mathcal{P}m}$ together with the pyramid outputs $f_{\mathcal{P}1}, f_{\mathcal{P}2}, f_{\mathcal{P}3}$ feeds a transformer decoder that predicts N class-agnostic binary masks $\{m_i\}_{i=1}^N$. For each mask m_i , we obtain its embedding via masked average pooling, $z_i = \langle f, m_i \rangle$. We also extract auxiliary mask embeddings and pyramid features in the same manner. Following (Carion et al. 2020; Cheng, Schwing, and Kirillov 2021), Hungarian matching assigns predictions to ground-truth masks. Class logits are optimized with binary-cross-entropy loss $\mathcal{L}_{\mathrm{BCE}}$, and mask shapes with Dice loss $\mathcal{L}_{\mathrm{DICE}}$.

Prompt grounding. We train on CosmicMan-HQ, which provides BLIP-generated dense captions containing detailed hair and clothing attributes. For each image–caption pair $\{x^{(m)}, s^{(m)}\}_{m=1}^{B}$ in a batch of size B, we extract K_{phrase} key phrases (relevant nouns and adjectives) from $s^{(m)}$, yielding $\{p_k\}_{k=1}^{K_{\text{phrase}}}$. Each phrase p_k is formatted into a prompt (e.g., "a photo of a tan purse" or "person hair length is above shoulders") and embedded with OPENCLIP (\mathcal{T}) (Ilharco et al. 2021). Following (Xu et al. 2023), we apply a contrastive loss that aligns phrase embeddings $\mathcal{T}(p_k)$ with their corresponding mask embeddings z_i . The grounding loss \mathcal{L}_G over the batch is then computed as:

$$g(x^{(m)}, s^{(m)}) = \frac{1}{K} \sum_{k=1}^{K} \sum_{i=1}^{N} \mathbf{p}_{ik} \cdot \langle z_i, \mathcal{T}(p_k) \rangle,$$

$$\mathcal{L}_G = -\frac{1}{B} \sum_{m=1}^{B} \log \frac{e^{2 \cdot g_{mm}/\tau}}{\sum_{n=1}^{B} e^{g_{mn}/\tau} \cdot \sum_{n=1}^{B} e^{g_{nm}/\tau}}.$$
(4)

Here, \mathbf{p}_{ik} is the softmax probability that mask embedding z_i matches base phrase p_k , with N denoting the number of class-agnostic binary masks. The similarity between mask and text embeddings is given by $\langle z_i, \mathcal{T}(p_k) \rangle$. We use g_{mm} as a shorthand for $g(x^{(m)}, s^{(m)})$, the similarity score for the matched image-caption pair, while g_{mn} and g_{nm} denote cross-similarity scores within the batch— g_{mn} being the

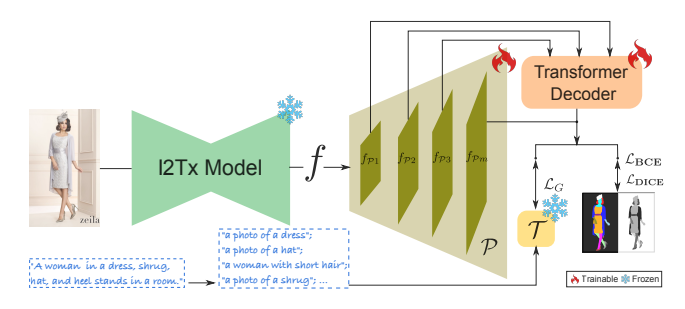


Figure 3: **Training.** Frozen I2Tx features from image x feed the pixel decoder \mathcal{P} and transformer, producing N classagnostic masks m optimized with \mathcal{L}_{BCE} and $\mathcal{L}_{\text{DICE}}$. Key prompt phrases, embedded by frozen \mathcal{T} , are contrastively aligned to m via \mathcal{L}_{G} .

similarity between the m-th image and other captions s^n , and g_{nm} the similarity between the m-th caption and other images x^n . τ is a learnable temperature parameter that scales the similarity scores. The total loss $\mathcal{L}_{\text{total}}$ is computed using weights λ_{BCE} , λ_{DICE} , and λ_{G} for \mathcal{L}_{BCE} , $\mathcal{L}_{\text{DICE}}$, and \mathcal{L}_{G} , respectively. See Sup. Mat. for definitions of $\mathcal{L}_{\text{DICE}}$ and \mathcal{L}_{BCE} .

$$\mathcal{L}_{\text{total}} = \lambda_{\text{BCE}} \mathcal{L}_{\text{BCE}} + \lambda_{\text{DICE}} \mathcal{L}_{\text{DICE}} + \lambda_{\text{G}} \mathcal{L}_{\text{G}}.$$
 (5)

Implementation Details

I2Tx model. We use CLIP-VIT-H/14 (trained on the 224×224 LAION-2B English subset of LAION-5B (Schuhmann et al. 2022b)) as the base CLIP-VISION model. Tex-Dreamer trains an IM2CONTEXT model (linear projection + 3-layer Transformer decoder; visual/text dims: 1280/1024) and fine-tunes CLIP-VISION (scaling factor $\alpha = 16$, rank r=16) and SD ($\alpha=128, r=128$) with LoRA, all on the ATLAS dataset (Liu et al. 2024) (50K 1024×1024 3D human textures in SMPL UV space (Loper et al. 2023)). We merge the LoRA adapters into CLIP-VISION and the texture-finetuned SD UNet via Diffusers (von Platen et al. 2022), using a diffusion time step of 0, a 256-dimensional latent, and seed 777. Captions are processed by extracting $K_{\text{phrase}} = 9 \text{ nouns/adjectives with NLTK (Bird, Klein, and}$ Loper 2009), and text embeddings come from VIT-H/14 OPENCLIP (Ilharco et al. 2021).

Semantic parsing. I2Tx features are upsampled via MS-DEFORMATTN (Zhu et al. 2021). The transformer decoder (8 heads, 9 layers) predicts N=100 class-agnostic binary masks and dynamically assigns unique colors to each mask for body parts and clothing.

Datasets. We train on 100K images randomly drawn from 27 parquet files (514K total) in Laion2B-en and Laion1B-nolang (CosmicMan-HQ subset of LAION-5B (Schuhmann et al. 2022a)), yielding 6M images overall, obtained via img2dataset (Beaumont 2021) tool. Seventeen base categories are listed in table 4, and GT masks are resized to the original image size during training.

Training details. Images are augmented with horizontal/vertical flips and resized to 1024; test images keep aspect ratio with the shorter edge at 1024. Loss weights are

Table 1: Human parsing on CosmicManHQ (test) and GranD-f (cross) under COP and BHP. M2F-C_{close} and ODISE-C_{open} are retrained on our CosmicManHQ split. Best scores are highlighted in teal, second best in gray.

			Cosmic	ManHQ					Cross-datas	et: GranD	-f	
Method		COP			BHP			COP			BHP	
	mIoU	mAcc	mAP ^{SS}	mIoU	mAcc	mAP ^{SS}	mIoU	mAcc	mAP ^{SS}	mIoU	mAcc	mAP ^{SS}
PPP-SCHP (Mottaghi et al. 2014b)			_	45.2	49.7	34.0	_		_	20.4	22.4	15.3
ATR-SCHP (Liang et al. 2015)	44.3	48.7	34.0	50.2	55.4	37.6	19.5	21.4	14.7	22.8	25.1	17.2
LIP-SCHP (Gong et al. 2017)	42.0	45.4	31.1	46.6	50.8	34.7	18.5	20.3	13.9	21.6	23.7	16.2
CIHP-PGN (Gong et al. 2018a)	43.1	47.1	30.6	48.4	53.1	37.1	19.0	20.8	13.3	22.2	23.4	16.0
Sapiens-1B (Khirodkar et al. 2024)	52.4	57.1	40.3	58.5	62.2	42.1	25.1	27.3	18.4	27.5	30.5	20.5
M2F-C _{close} (Cheng et al. 2022b)	49.7	54.4	33.6	54.1	57.2	34.1	24.8	26.9	17.6	25.0	27.0	18.0
ODISE-C _{open} (Xu et al. 2023)	65.7	72.2	49.3	73.4	77.0	53.7	21.5	17.2	12.2	23.5	19.2	14.2
Ours	77.5	79.4	58.2	86.3	88.2	65.1	27.1	29.8	21.0	30.2	33.1	22.9

 $\lambda_{\rm BCE}=2.0, \lambda_{\rm DICE}=5.0, \lambda_{\rm G}=1.0.$ Following (Cheng et al. 2022a), mask loss is computed on 112×112 (12,544) random points from matched mask pairs. We use AdamW with a 1e-4 learning rate and 0.05 weight decay. The model has 2.005B parameters (29.55M or 0.86% trainable) and trains for about 12.2 days (370K iterations, batch size 8) on eight A100 GPUs. Inference runs on a single 32 GB V100 GPU.

Experiments Evaluation settings. We assess Spectrum under four tasks

(see fig. 4): FPP-Full-Person Parsing (one mask per person), BHP-Bare-Human Parsing (body part masks), CCP—COCO Category Parsing (accessories: backpack, umbrella, shoe, eye glasses, handbag, tie, suitcase), and COP—Clothing-Only Parsing (one mask per clothing). To ensure fair comparison, we unify baseline labels by relabelling equivalent categories (e.g., pants bottoms, upper/lower arms hand) and ignore classes a baseline was never trained to predict. Spectrum outputs BHP, CCP, and COP masks, which we merge to form an FPP mask for comparison. All scores use pixel-wise agreement with the GT. Cross-dataset evaluation. The model is trained on singlehuman CosmicManHQ (Li et al. 2024) and tested on its hold-out split, on GranD-f (Rasheed et al. 2024) (multihuman, all four settings), and on standard human parsing datasets ATR (Liang et al. 2015), LIP (Gong et al. 2017), PPP (Mottaghi et al. 2014b), and CIHP (Gong et al. 2018a). GranD-f poses challenging crowded scenes, heavy occlusion, and incomplete GT masks—resulting in lower absolute scores for all methods. The prompts follow the original annotations (CosmicManHQ: BLIP (Li et al. 2022b); GranD-f: Vicuna (Chiang et al. 2023)); the lengthy captions are compressed while retaining every clothing term. Qualitative figures show the prompt (teal) and the extended body-parts list (EBP); the full EBP is face, faces, hand, hands, hair, hairs, wavy, ponytail, bob, bald, curly, afro-hair, leg, legs, back, chest, belly, stomach, and feet.

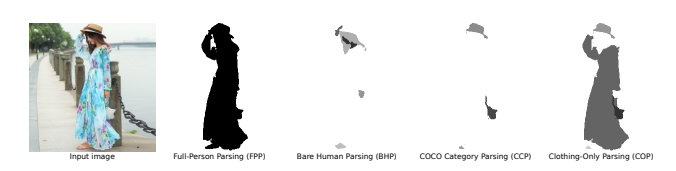


Figure 4: FPP, BHP, CCP, and COP masks.



Figure 5: Standard parsers (R2–4); w/o \mathcal{L}_G ablation (R5).

Closed-set Segmentors

We benchmark Spectrum against state of the art human-parsing models that assume a fixed label set (BHP and COP only). Specifically, we compare against (i) the original Sapiens-1B (Khirodkar et al. 2024) and CIHP-PGN (Gong et al. 2018a); (ii) three SCHP (Li et al. 2022d) variants retrained on the standard ATR, LIP, and PPP human parsing datasets; and (iii) two models trained on our Cosmic-ManHQ split—Mask2Former in a closed-set setting (M2F-C_{close}) (Cheng et al. 2022b) and the open-vocabulary segmentor ODISE-C (Xu et al. 2023). (PPP-SCHP outputs BHP masks only due to label mismatches with COP.) Ta-



Figure 6: (Left) **Multihuman GranD-f**: ours surpasses Sapiens-1B and retrained ODISE-C. (Right) **Open-vocabulary parsing in the wild**: baselines merge all people into one mask, whereas ours preserves distinct clothing and body-part masks.

ble 1 reports results on the CosmicManHQ test split and on GranD-f (Rasheed et al. 2024). Each COP/BHP entry lists (mIoU, mAcc, mAPSS@0.5-0.95). Spectrum outperforms all baselines in every metric; Sapiens-1B ranks second, while ODISE-C, though open-vocabulary, still falls short. Cross-dataset results in table 5b show that our method achieves higher mIoU than the three SCHP variants on their respective training datasets (LIP, ATR, and PPP) and also surpasses the PGN baseline on CIHP, highlighting its strong generalization ability. Qualitative comparisons in fig. 5 (rows 1-4) reflect this trend: Spectrum delivers complete, semantically correct masks for all visible body parts and novel garments (wedding dress, skirt, shirt), dynamically assigning new colours (e.g., different colours for multiple hands). In comparison, Sapiens-1B and other baselines show fragmented regions (yellow box highlight). See the Sup. Mat. for dynamic-colour mask assignments.

Open-vocabulary Segmentors

Most open-vocabulary models output a single *person* mask (FPP) and lack BHP support; we therefore evaluate them

Table 2: **Open-vocabulary semantic parsing.** † indicates diffusion-based methods; * indicates CLIP-based methods.

Method	Cosm	ucManHQ		Cross data: GranD-f – COP					
Method	mIoU	mAcc	mAP ^{SS}	mIoU	mAcc	mAP ^{SS}			
GD [†] (Li et al. 2023)	14.6	18.0	11.5	7.6	9.8	6.5			
IFSeg (Yun et al. 2023)	32.0	35.2	24.1	13.7	15.0	10.4			
MCLIP* (Zheng Ding 2023)	29.1	32.0	21.9	13.2	14.5	10.0			
ODISE [†] (Xu et al. 2023)	33.3	36.6	25.1	14.0	15.4	10.6			
OVSeg* (Liang et al. 2023)	25.6	27.5	19.3	12.8	14.1	9.7			
OVAM [†] (Manchón et al. 2024)	25.6	29.5	19.3	8.5	11.8	7.9			
SED (Xie et al. 2024)	44.0	48.4	33.1	14.6	16.8	11.0			
SEEM (Zou et al. 2023)	29.8	36.0	21.4	11.4	12.8	9.9			
LISA (Lai et al. 2024)	40.5	44.0	30.4	15.2	17.7	10.9			
Ours [†]	77.5	79.4	58.2	27.1	29.8	21.0			

only under COP. Semantic segmentation. We benchmark IFSeg (Yun et al. 2023), MCLIP (Zheng Ding 2023), OVSeg (Liang et al. 2023), SED (Xie et al. 2024), SEEM (Zou et al. 2023), LISA (Lai et al. 2024), and the T2I-based GD (Li et al. 2023), OVAM (Manchón et al. 2024), and ODISE (Xu et al. 2023). Instance segmentation. We include GGN (Wang et al. 2022), OLN (Kim et al. 2022b), MCLIP, and ODISE. Table 2 lists COP scores—(mIoU, mAcc, mAPSS@0.5-0.95)—on the CosmicManHQ test split and on GranD-f; Spectrum outperforms all semantic baselines, with SED and LISA closest. Table 3 reports instance metrics (mAPIS@0.5-0.95, AR@100); Spectrum again leads by a wide margin (GGN, OLN cannot output COP masks). Qualitative comparisons in fig. 6 show complex multi-human scenes from GranD-f (left) and in-the-wild images (right). Spectrum yields coherent masks for every garment and body part, whereas parsing baselines (Sapiens-1B, ODISE-C) fragment garments and open-vocabulary segmentors (ODISE, OVSeg) often collapse all people into one mask (highlighted in yellow boxes). We also tested SAM 2 (Ravi et al. 2025) with point prompts on a small subset; results are shown qualitatively only, as its task setting is not directly comparable.

Table 3: Open-vocabulary instance parsing.

	ı	Cosmic	ManHQ		Cross-dataset: GranD-f								
Method	COP		FPP			OP	FPP						
	mAP ^{IS}	AR@100	mAP ^{IS}	AR@100	mAP ^{IS}	AR@100	mAP ^{IS}	AR@100					
GGN			20.4	33.0	_		11.7	26.3					
MCLIP*	3.9	6.0	27.8	39.4	2.2	5.4	19.5	29.2					
OLN	l —	_	23.6	30.7	_	_	11.3	24.7					
$ODISE^{\dagger}$	4.2	7.7	36.5	59.5	3.6	6.9	22.9	30.1					
Ours [†]	24.7	30.3	42.4	66.1	17.1	26.2	31.2	39.8					

Table 4: **Per-class IoU** (%) **for Spectrum and ablations** (w/o C, \mathcal{L}_G , f). L/R subscripts indicate left/right parts.

Model	Face	$_L$ Ha	nd_R	Hair	Bags	Special Clothings	Tops	Eyewear	$_L$ Le	eg_R	Hats	Belts	$_L$ Sh	oe_R	One-piece Outfits	Scarf	Bottoms	Avg
w/o C	16.71	19.63	16.46	15.11	18.5	11.59	17.48	19.58	15.19	16.12	18.81	13.91	18.11	16.19	17.07	19.43	18.93	16.99
w/o \mathcal{L}_G	52.99	62.24	52.2	47.91	58.67	36.76	55.43	62.09	48.18	51.13	59.67	44.1	57.44	51.35	54.14	61.61	60.05	53.88
w/o f	66.25	77.82	65.26	59.9	73.35	45.95	69.3	77.63	60.23	63.93	74.59	55.13	71.82	64.2	67.68	77.02	75.07	67.36
Ours	84.47	91.22	83.21	84.37	93.52	62.59	88.36	94.98	76.8	81.51	95.11	72.3	91.57	81.86	86.3	96.21	95.72	85.89

Table 5: Unseen/seen and cross-dataset mIoU evaluation.

(a) Unseen (U)/ Seen (S) COP

(b) Cross-dataset Eval.

Method	Cos	mic	Gra	nD-f					
Method	U	S	U	U S Method		LIP	ATR	PPP	CIHP
ODISE	24.6	38.5	7.7	18.1	SCHP	59.36	82.29	71.46	-
ODISE-C	51.2	69.0	15.2	23.3	PGN	-	-	-	55.8
Ours	60.8	80.8	18.9	29.9	Ours	85.6	85.9	82.5	80.3

Table 6: Model size analysis.

Method	FPS	GFLOPS	#Params
OVSeg (Liang et al. 2023)	1.1	0.830	531M
ODISE (Xu et al. 2023)	0.6	0.953	1522M
MCLIP (Zheng Ding 2023)	2.5	0.542	367M
Ours	0.5	0.976	1571M

Unseen Clothing

Because closed-set parsers cannot handle novel classes, we evaluate only open-vocabulary models under COP, separating seen vs. unseen clothing. A BERT-NER filter (Devlin et al. 2019; Tjong Kim Sang and De Meulder 2003) removes test-set labels that overlap the training set, leaving categories such as *maxi*, *floral shirt*, *jumpsuit*, *loafers*, *sneakers*, *polo shirt*, *midi*, *camisole*, *hoodie*, *leather jacket*, *slippers*, *military dress*, *saree*, *baby dress*, *jersey*, *fur coat*, *brief*, *bandana*, etc. Table 5a reports mIoU on CosmicManHQ and GranD-f for unseen/seen COP splits, comparing Spectrum with two top-performing baselines, ODISE and retrained ODISE-C. Spectrum achieves the highest scores, with ODISE-C second. Qualitative examples in figs. 1, 5 and 6 further show accurate masks on novel clothing, thanks to the repurposed I2Tx features and prompt grounding.

Model Size Analysis

Table 6 reports FPS, GFLOPs, and parameters for Spectrum, OVSeg, ODISE, and MCLIP. Although Spectrum is not efficiency-focused, its runtime and compute load are close to ODISE, while MCLIP have the smallest footprint.

Ablation studies

We ablate Spectrum modules on the CosmicManHQ test split and report mIoU; per-class IoU is in table 4. Additional FPP/CCP metrics, qualitative single- and multi-human examples, prompt variants, failure cases, limitations, and ethical notes appear in the Sup. Mat.

Standard SD features. Substituting our I2Tx texture features with vanilla SD latent features reduces mIoU to 67.36, showing that texture-aligned latents are substantially more informative for diverse clothing and body-part parsing.

Without context embedding (C and CLS). Removing the context embedding drops mIoU from 85.89 to 16.99, as it

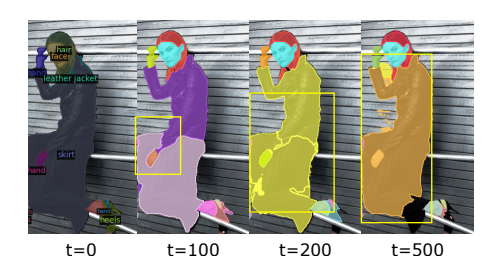


Figure 7: **Ablation—diffusion timesteps.** Parsing at t = 0, 100, 200, 500; t = 0 performs best.

provides essential conditioning for the I2Tx model.

Without grounding loss (\mathcal{L}_G). Omitting the contrastive prompt-grounding loss drops mIoU to 53.88 and causes clothing to collapse to generic *Special Clothing* label (fig. 5 R5), highlighting the importance of prompt alignment.

Diffusion timesteps. We extract I2Tx features in a single forward pass at t=0, skipping denoising. Sampling $t \in \{100, 200, 500\}$ from the 1000-step schedule yields fragmented masks and poorer segmentation (fig. 7).

Low exposure ablation. Our training data (CosmicManHQ split) and ATLAS 3D textures are well lit, so darker scenes create a domain gap. Applying gamma correction ($0 < \gamma < 1$) to simulate under-exposure drops mIoU to 79.11 at $\gamma = 0.75$, 54.20 at $\gamma = 0.50$, and 30.90 at $\gamma = 0.25$, showing that low light markedly harms performance.

Conclusion

We present Spectrum, a unified network for part-level pixel parsing of diverse clothing and body parts, as well as instance-level part grouping. It leverages the internal representation of an I2Tx diffusion model—trained to align 3D textures with input images—to generate accurate segmentation maps for visible body parts and clothing categories, while ignoring standalone garments and irrelevant objects. Extensive cross-dataset experiments, including single and multi-human scenarios, evaluate body parts, clothing parts, unseen categories, and full-body masks. Spectrum consistently outperforms state-of-the-art human parsers, openvocabulary segmentors, and instance segmentation baselines in prompt-based mask prediction. In particular, it achieves superior generalization to unseen clothing categories in cross-dataset settings. These findings suggest that repurposing 3D texture features from fine-tuned diffusion models can support more detailed and generalizable human parsing.

Acknowledgments and disclosure. We thank Michael Black for valuable feedback. We also thank Zitian Zhang for proofreading and insightful discussions. This work was conducted during an internship at Adobe Research.

References

- Amit, T.; Shaharbany, T.; Nachmani, E.; and Wolf, L. 2022. SegDiff: Image Segmentation with Diffusion Probabilistic Models. arXiv:2112.00390.
- Beaumont, R. 2021. Img2dataset: Easily turn large sets of image urls to an image dataset. https://github.com/rom1504/img2dataset.
- Bendale, A.; and Boult, T. 2015. Towards Open World Recognition. In *IEEE Conf. Comput. Vis. Pattern Recog.* IEEE.
- Bird, S.; Klein, E.; and Loper, E. 2009. *Natural language processing with Python: analyzing text with the natural language toolkit.* "O'Reilly Media, Inc.".
- Carion, N.; Massa, F.; Synnaeve, G.; Usunier, N.; Kirillov, A.; and Zagoruyko, S. 2020. End-to-End Object Detection with Transformers. In Vedaldi, A.; Bischof, H.; Brox, T.; and Frahm, J., eds., *Eur. Conf. Comput. Vis.*, volume 12346 of *Lecture Notes in Computer Science*, 213–229. Springer.
- Casas, D.; and Comino-Trinidad, M. 2023. SMPLitex: A Generative Model and Dataset for 3D Human Texture Estimation from Single Image. In *Brit. Mach. Vis. Conf.*
- Chen, L.; Papandreou, G.; Kokkinos, I.; Murphy, K.; and Yuille, A. L. 2018. DeepLab: Semantic Image Segmentation with Deep Convolutional Nets, Atrous Convolution, and Fully Connected CRFs. *IEEE Trans. Pattern Anal. Mach. Intell.*, 40(4): 834–848.
- Chen, L.; Yang, Y.; Wang, J.; Xu, W.; and Yuille, A. L. 2016. Attention to Scale: Scale-Aware Semantic Image Segmentation. In *IEEE Conf. Comput. Vis. Pattern Recog.*, 3640–3649. IEEE Computer Society.
- Chen, T.; Li, L.; Saxena, S.; Hinton, G. E.; and Fleet, D. J. 2023. A Generalist Framework for Panoptic Segmentation of Images and Videos. In *Int. Conf. Comput. Vis.*, 909–919. IEEE.
- Chen, X.; Shrivastava, A.; and Gupta, A. 2014. Enriching Visual Knowledge Bases via Object Discovery and Segmentation. In *IEEE Conf. Comput. Vis. Pattern Recog.*, 2035–2042.
- Cheng, B.; Misra, I.; Schwing, A. G.; Kirillov, A.; and Girdhar, R. 2022a. Masked-attention Mask Transformer for Universal Image Segmentation. In *IEEE Conf. Comput. Vis. Pattern Recog.*, 1280–1289. IEEE.
- Cheng, B.; Misra, I.; Schwing, A. G.; Kirillov, A.; and Girdhar, R. 2022b. Masked-attention Mask Transformer for Universal Image Segmentation.
- Cheng, B.; Schwing, A. G.; and Kirillov, A. 2021. Per-Pixel Classification is Not All You Need for Semantic Segmentation. In Ranzato, M.; Beygelzimer, A.; Dauphin, Y. N.; Liang, P.; and Vaughan, J. W., eds., *Adv. Neural Inform. Process. Syst.*, 17864–17875.
- Chiang, W.-L.; Li, Z.; Lin, Z.; Sheng, Y.; Wu, Z.; Zhang, H.; Zheng, L.; Zhuang, S.; Zhuang, Y.; Gonzalez, J. E.; Stoica, I.; and Xing, E. P. 2023. Vicuna: An Open-Source Chatbot Impressing GPT-4 with 90%* ChatGPT Quality.

- Dai, J.; He, K.; and Sun, J. 2015. BoxSup: Exploiting Bounding Boxes to Supervise Convolutional Networks for Semantic Segmentation. In *Int. Conf. Comput. Vis.*, 1635–1643. IEEE Computer Society.
- Devlin, J.; Chang, M.; Lee, K.; and Toutanova, K. 2019. BERT: Pre-training of Deep Bidirectional Transformers for Language Understanding. In Burstein, J.; Doran, C.; and Solorio, T., eds., *Conf. of the North American Chapter of the Association for Computational Linguistics: Human Language Technologies*, 4171–4186. Association for Computational Linguistics.
- Dickens, J.; and Hamad, K. 2025. Part Segmentation of Human Meshes via Multi-View Human Parsing. arXiv:2507.18655.
- Dong, J.; Chen, Q.; Shen, X.; Yang, J.; and Yan, S. 2014. Towards Unified Human Parsing and Pose Estimation. In *IEEE Conf. Comput. Vis. Pattern Recog.*, 843–850.
- Esser, P.; Kulal, S.; Blattmann, A.; Entezari, R.; Müller, J.; Saini, H.; Levi, Y.; Lorenz, D.; Sauer, A.; Boesel, F.; Podell, D.; Dockhorn, T.; English, Z.; and Rombach, R. 2024. Scaling Rectified Flow Transformers for High-Resolution Image Synthesis. In *Int. Conf. on Machine Learning*. OpenReview.net.
- Fang, H.; Lu, G.; Fang, X.; Xie, J.; Tai, Y.; and Lu, C. 2018. Weakly and Semi Supervised Human Body Part Parsing via Pose-Guided Knowledge Transfer. In *IEEE Conf. Comput. Vis. Pattern Recog.*, 70–78.
- Gan, C.; Lin, M.; Yang, Y.; Melo, G. d.; and Hauptmann, A. G. 2016. Concepts not alone: exploring pairwise relationships for zero-shot video activity recognition. In *AAAI Conf. on Artificial Intelligence*, AAAI'16, 3487–3493.
- Geng, C.; Huang, S.-J.; and Chen, S. 2021. Recent Advances in Open Set Recognition: A Survey. *IEEE Trans. Pattern Anal. Mach. Intell.*, 43(10): 3614–3631.
- Ghiasi, G.; Gu, X.; Cui, Y.; and Lin, T. 2022a. Scaling Open-Vocabulary Image Segmentation with Image-Level Labels. In Avidan, S.; Brostow, G. J.; Cissé, M.; Farinella, G. M.; and Hassner, T., eds., *Eur. Conf. Comput. Vis.*, volume 13696 of *Lecture Notes in Computer Science*, 540–557. Springer.
- Ghiasi, G.; Gu, X.; Cui, Y.; and Lin, T.-Y. 2022b. Scaling Open-Vocabulary Image Segmentation with Image-Level Labels. In *Eur. Conf. Comput. Vis.*, 540–557. Berlin, Heidelberg: Springer-Verlag. ISBN 978-3-031-20058-8.
- Gkioxari, G.; Girshick, R. B.; and Malik, J. 2015. Actions and Attributes from Wholes and Parts. In *Int. Conf. Comput. Vis.*, 2470–2478. IEEE Computer Society.
- Gong, K.; Liang, X.; Li, Y.; Chen, Y.; Yang, M.; and Lin, L. 2018a. Instance-Level Human Parsing via Part Grouping Network. In Ferrari, V.; Hebert, M.; Sminchisescu, C.; and Weiss, Y., eds., *Eur. Conf. Comput. Vis.*, volume 11208 of *Lecture Notes in Computer Science*, 805–822. Springer.
- Gong, K.; Liang, X.; Li, Y.; Chen, Y.; Yang, M.; and Lin, L. 2018b. Instance-Level Human Parsing via Part Grouping Network. In Ferrari, V.; Hebert, M.; Sminchisescu, C.; and Weiss, Y., eds., *Eur. Conf. Comput. Vis.*, 805–822. Cham: Springer International Publishing. ISBN 978-3-030-01225-0.

- Gong, K.; Liang, X.; Zhang, D.; Shen, X.; and Lin, L. 2017. Look into Person: Self-Supervised Structure-Sensitive Learning and a New Benchmark for Human Parsing. In *IEEE Conf. Comput. Vis. Pattern Recog.*, 6757–6765. IEEE Computer Society.
- Gupta, A.; Wu, J.; Deng, J.; and Fei-Fei, L. 2023. Siamese Masked Autoencoders. In *Adv. Neural Inform. Process. Syst.*
- Ho, J.; Jain, A.; and Abbeel, P. 2020. Denoising diffusion probabilistic models. In *Adv. Neural Inform. Process. Syst.*
- Hu, E. J.; yelong shen; Wallis, P.; Allen-Zhu, Z.; Li, Y.; Wang, S.; Wang, L.; and Chen, W. 2022. LoRA: Low-Rank Adaptation of Large Language Models. In *Int. Conf. Learn. Represent.*
- Ilharco, G.; Wortsman, M.; Wightman, R.; Gordon, C.; Carlini, N.; Taori, R.; Dave, A.; Shankar, V.; Namkoong, H.; Miller, J.; Hajishirzi, H.; Farhadi, A.; and Schmidt, L. 2021. OpenCLIP.
- Ji, Y.; Chen, Z.; Xie, E.; Hong, L.; Liu, X.; Liu, Z.; Lu, T.; Li, Z.; and Luo, P. 2023. DDP: Diffusion Model for Dense Visual Prediction. In *Int. Conf. Comput. Vis.*, 21684–21695. IEEE.
- Jia, C.; Yang, Y.; Xia, Y.; Chen, Y.; Parekh, Z.; Pham, H.; Le, Q. V.; Sung, Y.; Li, Z.; and Duerig, T. 2021. Scaling Up Visual and Vision-Language Representation Learning With Noisy Text Supervision. In Meila, M.; and Zhang, T., eds., *Int. Conf. on Machine Learning*, volume 139 of *Proceedings of Machine Learning Research*, 4904–4916. PMLR.
- Khirodkar, R.; Bagautdinov, T. M.; Martinez, J.; Zhaoen, S.; James, A.; Selednik, P.; Anderson, S.; and Saito, S. 2024. Sapiens: Foundation for Human Vision Models. In Leonardis, A.; Ricci, E.; Roth, S.; Russakovsky, O.; Sattler, T.; and Varol, G., eds., *Eur. Conf. Comput. Vis.*, volume 15062 of *Lecture Notes in Computer Science*, 206–228. Springer.
- Kim, D.; Lin, T.; Angelova, A.; Kweon, I. S.; and Kuo, W. 2022a. Learning Open-World Object Proposals Without Learning to Classify. *IEEE Robotics Autom. Lett.*, 7(2): 5453–5460.
- Kim, D.; Lin, T.-Y.; Angelova, A.; Kweon, I. S.; and Kuo, W. 2022b. Learning Open-World Object Proposals without Learning to Classify. *IEEE Robotics and Autom. Lett.*
- Ladický, L.; Torr, P. H.; and Zisserman, A. 2013. Human Pose Estimation Using a Joint Pixel-wise and Part-wise Formulation. In *IEEE Conf. Comput. Vis. Pattern Recog.*, 3578–3585.
- Lai, X.; Tian, Z.; Chen, Y.; Li, Y.; Yuan, Y.; Liu, S.; and Jia, J. 2024. LISA: Reasoning Segmentation via Large Language Model. In *IEEE Conf. Comput. Vis. Pattern Recog.*, 9579–9589. IEEE.
- Li, D.; Ling, H.; Kim, S. W.; Kreis, K.; Fidler, S.; and Torralba, A. 2022a. BigDatasetGAN: Synthesizing ImageNet with Pixel-wise Annotations. In *IEEE Conf. Comput. Vis. Pattern Recog.*, 21298–21308. IEEE.
- Li, J.; Li, D.; Xiong, C.; and Hoi, S. C. H. 2022b. BLIP: Bootstrapping Language-Image Pre-training for Unified Vision-Language Understanding and Generation. In

- Chaudhuri, K.; Jegelka, S.; Song, L.; Szepesvári, C.; Niu, G.; and Sabato, S., eds., *Int. Conf. on Machine Learning*, volume 162 of *Proceedings of Machine Learning Research*, 12888–12900. PMLR.
- Li, J.; Zhao, J.; Wei, Y.; Lang, C.; Li, Y.; Sim, T.; Yan, S.; and Feng, J. 2017. Multi-Human Parsing in the Wild. *arXiv* preprint arXiv:1705.07206.
- Li, L.; Zhou, T.; Wang, W.; Yang, L.; Li, J.; and Yang, Y. 2022c. Locality-Aware Inter-and Intra-Video Reconstruction for Self-Supervised Correspondence Learning. In *IEEE Conf. Comput. Vis. Pattern Recog.*
- Li, P.; Xu, Y.; Wei, Y.; and Yang, Y. 2022d. Self-Correction for Human Parsing. *IEEE Trans. Pattern Anal. Mach. Intell.*, 44(6): 3260–3271.
- Li, S.; Fu, J.; Liu, K.; Wang, W.; Lin, K.; and Wu, W. 2024. CosmicMan: A Text-to-Image Foundation Model for Humans. In *IEEE Conf. Comput. Vis. Pattern Recog.*, 6955–6965. IEEE.
- Li, Z.; Zhou, Q.; Zhang, X.; Zhang, Y.; Wang, Y.; and Xie, W. 2023. Open-vocabulary Object Segmentation with Diffusion Models.
- Liang, F.; Wu, B.; Dai, X.; Li, K.; Zhao, Y.; Zhang, H.; Zhang, P.; Vajda, P.; and Marculescu, D. 2023. Open-Vocabulary Semantic Segmentation with Mask-adapted CLIP. In *IEEE Conf. Comput. Vis. Pattern Recog.*, 7061–7070. IEEE.
- Liang, X.; Liu, S.; Shen, X.; Yang, J.; Liu, L.; Dong, J.; Lin, L.; and Yan, S. 2015. Deep Human Parsing with Active Template Regression. *IEEE Trans. Pattern Anal. Mach. Intell.*, 37(12): 2402–2414.
- Lin, L.; Zhang, D.; Luo, P.; and Zuo, W. 2019. *Human Centric Visual Analysis with Deep Learning*. Springer Publishing Company, Incorporated, 1st edition. ISBN 9789811323867.
- Liu, K.; Choi, O.; Wang, J.; and Hwang, W. 2022. CDGNet: Class Distribution Guided Network for Human Parsing. In *IEEE Conf. Comput. Vis. Pattern Recog.*, 4473–4482.
- Liu, K.; Wang, J.; Jin, R.; Hwang, W.; and Chung, T.-S. 2025. SCHNet: SAM Marries CLIP for Human Parsing. arXiv:2503.22237.
- Liu, Y.; Zhu, J.; Tang, J.; Zhang, S.; Zhang, J.; Cao, W.; Wang, C.; Wu, Y.; and Huang, D. 2024. TexDreamer: Towards Zero-Shot High-Fidelity 3D Human Texture Generation. In Leonardis, A.; Ricci, E.; Roth, S.; Russakovsky, O.; Sattler, T.; and Varol, G., eds., *Eur. Conf. Comput. Vis.*, volume 15105 of *Lecture Notes in Computer Science*, 184–202. Springer.
- Long, J.; Shelhamer, E.; and Darrell, T. 2015. Fully convolutional networks for semantic segmentation. In *IEEE Conf. Comput. Vis. Pattern Recog.*, 3431–3440. IEEE Computer Society.
- Loper, M.; Mahmood, N.; Romero, J.; Pons-Moll, G.; and Black, M. J. 2023. *SMPL: A Skinned Multi-Person Linear Model*. New York, NY, USA: Association for Computing Machinery, 1 edition. ISBN 9798400708978.

- Lu, Y.; Boukharouba, K.; Boonært, J.; Fleury, A.; and Lecœuche, S. 2014. Application of an incremental SVM algorithm for on-line human recognition from video surveillance using texture and color features. *Neurocomputing*, 126: 132–140. Recent trends in Intelligent Data Analysis Online Data Processing.
- Luo, P.; Wang, X.; and Tang, X. 2013. Pedestrian Parsing via Deep Decompositional Network. *Int. Conf. Comput. Vis.*, 2648–2655.
- Luo, Y.; Zheng, Z.; Zheng, L.; Guan, T.; Yu, J.; and Yang, Y. 2018. Macro-Micro Adversarial Network for Human Parsing. In Ferrari, V.; Hebert, M.; Sminchisescu, C.; and Weiss, Y., eds., *Eur. Conf. Comput. Vis.*, volume 11213 of *Lecture Notes in Computer Science*, 424–440. Springer.
- Manchón, P. M.; Alcover-Couso, R.; SanMiguel, J. C.; and Martínez, J. M. 2024. Open-Vocabulary Attention Maps with Token Optimization for Semantic Segmentation in Diffusion Models. In *IEEE Conf. Comput. Vis. Pattern Recog.*, 9242–9252.
- Mao, J.; Xiao, T.; Jiang, Y.; and Cao, Z. 2017. What Can Help Pedestrian Detection? In *IEEE Conf. Comput. Vis. Pattern Recog.*, 6034–6043. IEEE Computer Society.
- Mottaghi, R.; Chen, X.; Liu, X.; Cho, N.; Lee, S.; Fidler, S.; Urtasun, R.; and Yuille, A. L. 2014a. The Role of Context for Object Detection and Semantic Segmentation in the Wild. In *IEEE Conf. Comput. Vis. Pattern Recog.*, 891–898. IEEE Computer Society.
- Mottaghi, R.; Chen, X.; Liu, X.; Cho, N.-G.; Lee, S.-W.; Fidler, S.; Urtasun, R.; and Yuille, A. 2014b. The Role of Context for Object Detection and Semantic Segmentation in the Wild. In *IEEE Conf. Comput. Vis. Pattern Recog.*
- Nichol, A. Q.; and Dhariwal, P. 2021. Improved Denoising Diffusion Probabilistic Models. In Meila, M.; and Zhang, T., eds., *Int. Conf. on Machine Learning*, volume 139 of *Proceedings of Machine Learning Research*, 8162–8171. PMLR.
- Nichol, A. Q.; Dhariwal, P.; Ramesh, A.; Shyam, P.; Mishkin, P.; McGrew, B.; Sutskever, I.; and Chen, M. 2022. GLIDE: Towards Photorealistic Image Generation and Editing with Text-Guided Diffusion Models. In Chaudhuri, K.; Jegelka, S.; Song, L.; Szepesvári, C.; Niu, G.; and Sabato, S., eds., *Int. Conf. on Machine Learning*, volume 162 of *Proceedings of Machine Learning Research*, 16784–16804. PMLR.
- Qian, R.; Ding, S.; Liu, X.; and Lin, D. 2023. Semantics meets temporal correspondence: Self-supervised object-centric learning in videos. In *Int. Conf. Comput. Vis.*, 16675–16687.
- Radford, A.; Kim, J. W.; Hallacy, C.; Ramesh, A.; Goh, G.; Agarwal, S.; Sastry, G.; Askell, A.; Mishkin, P.; Clark, J.; Krueger, G.; and Sutskever, I. 2021. Learning Transferable Visual Models From Natural Language Supervision. In Meila, M.; and Zhang, T., eds., *Int. Conf. on Machine Learning*, volume 139 of *Proceedings of Machine Learning Research*, 8748–8763. PMLR.
- Ramanathan, V.; Kalia, A.; Petrovic, V.; Wen, Y.; Zheng, B.; Guo, B.; Wang, R.; Marquez, A.; Kovvuri, R.; Kadian, A.;

- Mousavi, A.; Song, Y.; Dubey, A.; and Mahajan, D. 2023. PACO: Parts and Attributes of Common Objects. In *IEEE Conf. Comput. Vis. Pattern Recog.*, 7141–7151. IEEE.
- Rasheed, H. A.; Maaz, M.; Mullappilly, S. S.; Shaker, A. M.; Khan, S. H.; Cholakkal, H.; Anwer, R. M.; Xing, E. P.; Yang, M.; and Khan, F. S. 2024. GLaMM: Pixel Grounding Large Multimodal Model. In *IEEE Conf. Comput. Vis. Pattern Recog.*, 13009–13018. IEEE.
- Ravi, N.; Gabeur, V.; Hu, Y.; Hu, R.; Ryali, C.; Ma, T.; Khedr, H.; Rädle, R.; Rolland, C.; Gustafson, L.; Mintun, E.; Pan, J.; Alwala, K. V.; Carion, N.; Wu, C.; Girshick, R. B.; Dollár, P.; and Feichtenhofer, C. 2025. SAM 2: Segment Anything in Images and Videos. In *Int. Conf. Learn. Represent*. OpenReview.net.
- Rombach, R.; Blattmann, A.; Lorenz, D.; Esser, P.; and Ommer, B. 2022. High-Resolution Image Synthesis With Latent Diffusion Models. In *IEEE Conf. Comput. Vis. Pattern Recog.*, 10684–10695.
- Saharia, C.; Chan, W.; Saxena, S.; Li, L.; Whang, J.; Denton, E. L.; Ghasemipour, S. K. S.; Lopes, R. G.; Ayan, B. K.; Salimans, T.; Ho, J.; Fleet, D. J.; and Norouzi, M. 2022. Photorealistic Text-to-Image Diffusion Models with Deep Language Understanding. In Koyejo, S.; Mohamed, S.; Agarwal, A.; Belgrave, D.; Cho, K.; and Oh, A., eds., *Adv. Neural Inform. Process. Syst.*
- Schuhmann, C.; Beaumont, R.; Vencu, R.; Gordon, C.; Wightman, R.; Cherti, M.; Coombes, T.; Katta, A.; Mullis, C.; Wortsman, M.; Schramowski, P.; Kundurthy, S.; Crowson, K.; Schmidt, L.; Kaczmarczyk, R.; and Jitsev, J. 2022a. LAION-5B: An open large-scale dataset for training next generation image-text models. In Koyejo, S.; Mohamed, S.; Agarwal, A.; Belgrave, D.; Cho, K.; and Oh, A., eds., *Adv. Neural Inform. Process. Syst.*
- Schuhmann, C.; Beaumont, R.; Vencu, R.; Gordon, C. W.; Wightman, R.; Cherti, M.; Coombes, T.; Katta, A.; Mullis, C.; Wortsman, M.; Schramowski, P.; Kundurthy, S. R.; Crowson, K.; Schmidt, L.; Kaczmarczyk, R.; and Jitsev, J. 2022b. LAION-5B: An open large-scale dataset for training next generation image-text models. In *Adv. Neural Inform. Process. Syst.*
- Shen, X.; Gao, H.; Tao, X.; Zhou, C.; and Jia, J. 2017. High-Quality Correspondence and Segmentation Estimation for Dual-Lens Smart-Phone Portraits. In *Int. Conf. Comput. Vis.*, 3277–3286. IEEE Computer Society.
- Shen, X.; Tao, X.; Gao, H.; Zhou, C.; and Jia, J. 2016. Deep Automatic Portrait Matting. In *Eur. Conf. Comput. Vis.*
- Tjong Kim Sang, E. F.; and De Meulder, F. 2003. Introduction to the CoNLL-2003 Shared Task: Language-Independent Named Entity Recognition. In *Proceedings of the Seventh Conference on Natural Language Learning at HLT-NAACL* 2003, 142–147.
- Tu, M.; Ye, S.; Jung, H.; and Kim, J. 2025. SMPL-GPTexture: Dual-View 3D Human Texture Estimation using Text-to-Image Generation Models. arXiv:2504.13378.
- von Platen, P.; Patil, S.; Lozhkov, A.; Cuenca, P.; Lambert, N.; Rasul, K.; Davaadorj, M.; Nair, D.; Paul, S.; Berman, W.;

- Xu, Y.; Liu, S.; and Wolf, T. 2022. Diffusers: State-of-the-art diffusion models. https://github.com/huggingface/diffusers.
- Wang, C.; Wang, Y.; and Yuille, A. L. 2013. An Approach to Pose-Based Action Recognition. *IEEE Conf. Comput. Vis. Pattern Recog.*, 915–922.
- Wang, W.; Feiszli, M.; Wang, H.; Malik, J.; and Tran, D. 2022. Open-World Instance Segmentation: Exploiting Pseudo Ground Truth From Learned Pairwise Affinity. *IEEE Conf. Comput. Vis. Pattern Recog.*
- Wang, Y.; Tran, D.; Liao, Z.; and Forsyth, D. 2012. Discriminative Hierarchical Part-based Models for Human Parsing and Action Recognition. *Journal of Machine Learning Research*, 13(99): 3075–3102.
- Wu, J.; Li, X.; Xu, S.; Yuan, H.; Ding, H.; Yang, Y.; Li, X.; Zhang, J.; Tong, Y.; Jiang, X.; Ghanem, B.; and Tao, D. 2024. Towards Open Vocabulary Learning: A Survey. *IEEE Trans. Pattern Anal. Mach. Intell.*, 46(7): 5092–5113.
- Wu, Y.; Kirillov, A.; Massa, F.; Lo, W.-Y.; and Girshick, R. 2019. Detectron2. https://github.com/facebookresearch/detectron2.
- Xia, F.; Wang, P.; Chen, L.; and Yuille, A. L. 2016. Zoom Better to See Clearer: Human and Object Parsing with Hierarchical Auto-Zoom Net. In Leibe, B.; Matas, J.; Sebe, N.; and Welling, M., eds., *Eur. Conf. Comput. Vis.*, volume 9909 of *Lecture Notes in Computer Science*, 648–663. Springer.
- Xia, F.; Wang, P.; Chen, X.; and Yuille, A. L. 2017. Joint Multi-person Pose Estimation and Semantic Part Segmentation. In *IEEE Conf. Comput. Vis. Pattern Recog.*, 6080–6089. IEEE Computer Society.
- Xian, Y.; Lampert, C. H.; Schiele, B.; and Akata, Z. 2019. Zero-Shot Learning A Comprehensive Evaluation of the Good, the Bad and the Ugly. *IEEE Trans. Pattern Anal. Mach. Intell.*, 41(9): 2251–2265.
- Xie, B.; Cao, J.; Xie, J.; Khan, F. S.; and Pang, Y. 2024. SED: A Simple Encoder-Decoder for Open-Vocabulary Semantic Segmentation. In *IEEE Conf. Comput. Vis. Pattern Recog.*, 3426–3436. IEEE.
- Xu, J.; Liu, S.; Vahdat, A.; Byeon, W.; Wang, X.; and Mello, S. D. 2023. Open-Vocabulary Panoptic Segmentation with Text-to-Image Diffusion Models. In *IEEE Conf. Comput. Vis. Pattern Recog.*, 2955–2966. IEEE.
- Yang, J.; Wang, C.; Li, Z.; Wang, J.; and Zhang, R. 2023. Semantic Human Parsing via Scalable Semantic Transfer Over Multiple Label Domains. In *IEEE Conf. Comput. Vis. Pattern Recog.*, 19424–19433. IEEE.
- Yang, L.; Song, Q.; Wang, Z.; Hu, M.; Liu, C.; Xin, X.; Jia, W.; and Xu, S. 2020. Renovating Parsing R-CNN for Accurate Multiple Human Parsing. In *Eur. Conf. Comput. Vis.*
- Yuan, H.; Li, X.; Zhou, C.; Li, Y.; Chen, K.; and Loy, C. C. 2024. Open-Vocabulary SAM: Segment and Recognize Twenty-Thousand Classes Interactively. In *Eur. Conf. Comput. Vis.*, 419–437. Berlin, Heidelberg: Springer-Verlag. ISBN 978-3-031-72774-0.
- Yun, S.; Park, S. H.; Seo, P. H.; and Shin, J. 2023. IFSeg: Image-free Semantic Segmentation via Vision-Language Model. In *IEEE Conf. Comput. Vis. Pattern Recog.*

- Zhang, J.; Yang, J.; Wang, P.; Wang, H.; Lin, Y.; Zhang, H.; Sun, Y.; Du, X.; Li, Y.; Liu, Z.; Chen, Y.; and Li, H. 2024. OpenOOD v1.5: Enhanced Benchmark for Out-of-Distribution Detection. arXiv:2306.09301.
- Zhang, L.; Lin, L.; Liang, X.; and He, K. 2016. Is Faster R-CNN Doing Well for Pedestrian Detection? In Leibe, B.; Matas, J.; Sebe, N.; and Welling, M., eds., *Eur. Conf. Comput. Vis.*, volume 9906 of *Lecture Notes in Computer Science*, 443–457. Springer.
- Zhang, S.; Cao, X.; Qi, G.-J.; Song, Z.; and Zhou, J. 2022. AIParsing: Anchor-free instance-level human parsing. *IEEE Trans. Image Process.*, 31: 5599–5612.
- Zhang, Y.; Ling, H.; Gao, J.; Yin, K.; Lafleche, J.; Barriuso, A.; Torralba, A.; and Fidler, S. 2021. DatasetGAN: Efficient Labeled Data Factory With Minimal Human Effort. In *IEEE Conf. Comput. Vis. Pattern Recog.*, 10145–10155. Computer Vision Foundation / IEEE.
- Zheng, Z.; Yang, X.; Yu, Z.; Zheng, L.; Yang, Y.; and Kautz, J. 2019. Joint discriminative and generative learning for person re-identification. *IEEE Conf. Comput. Vis. Pattern Recog.*
- Zheng Ding, Z. T., Jieke Wang. 2023. Open-Vocabulary Universal Image Segmentation with MaskCLIP. In *International Conference on Machine Learning*.
- Zhou, B.; Zhao, H.; Puig, X.; Fidler, S.; Barriuso, A.; and Torralba, A. 2017. Scene Parsing Through ADE20K Dataset. In *IEEE Conf. Comput. Vis. Pattern Recog.*
- Zhou, Q.; Liang, X.; Gong, K.; and Lin, L. 2018. Adaptive Temporal Encoding Network for Video Instance-level Human Parsing. In *ACM Int. Conf. Multimedia*, MM '18, 1527–1535. Association for Computing Machinery.
- Zhu, C.; and Chen, L. 2024. A Survey on Open-Vocabulary Detection and Segmentation: Past, Present, and Future. *IEEE Trans. Pattern Anal. Mach. Intell.*, 46(12): 8954–8975. Zhu, S.; Fidler, S.; Urtasun, R.; Lin, D.; and Loy, C. C. 2017. Be Your Own Prada: Fashion Synthesis with Structural Coherence. In *Int. Conf. Comput. Vis.*, 1689–1697. IEEE Computer Society.
- Zhu, X.; Su, W.; Lu, L.; Li, B.; Wang, X.; and Dai, J. 2021. Deformable DETR: Deformable Transformers for End-to-End Object Detection. In *Int. Conf. Learn. Represent.* Open-Review.net.
- Zou, X.; Yang, J.; Zhang, H.; Li, F.; Li, L.; Wang, J.; Wang, L.; Gao, J.; and Lee, Y. J. 2023. Segment Everything Everywhere All at Once. In Oh, A.; Naumann, T.; Globerson, A.; Saenko, K.; Hardt, M.; and Levine, S., eds., *Adv. Neural Inform. Process. Syst.*

Appendix

The supplementary material provides full FPP and CCP results; definitions of the supervision losses; details on prompt variants and ensembling; extra qualitative examples—including dynamic mask-colour assignment, single and multi-human scenes, and challenging cases—and a discussion of limitations and ethical considerations.

Method	Method Training Details			CosmicManHQ						Cross-dataset: GranD-f					
	Cats.	Data	Supv.	F	FPP			CCP			FPP			CCP	
PPP-SCHP (Mottaghi et al. 2014b)	7	PPP (Mottaghi et al. 2014b)	ML		_			_			_			_	
ATR-SCHP (Liang et al. 2015)	18	ATR (Liang et al. 2015)	ML		_		47.3	52.1	35.8		_		21.2	23.3	16.0
LIP-SCHP (Gong et al. 2017)	20	LIP (Gong et al. 2017)	ML		_		44.3	48.1	32.9		_		20.1	22.0	15.1
CIHP-PGN (Gong et al. 2018a)	20	CIHP (Gong et al. 2018a)	ML		_		45.6	50.4	34.0		_		20.7	22.7	15.6
Sapiens-1B (Khirodkar et al. 2024)	20,28	H{300M,2K} (Khirodkar et al. 2024)	ML		_		55.5	59.5	41.0		_		26.3	29.3	19.3
M2F-C _{close} (Cheng et al. 2022b)	17	CMHQ (Li et al. 2024)	MC		_		51.5	55.5	33.5		_		24.5	26.5	17.5
ODISE-C [†] open (Xu et al. 2023)	17	CMHQ (Li et al. 2024)	MCG	80.8 8	81.6	57.9	69.5	74.1	50.7	24.3	20.1	15.3	22.1	18.2	13.1
GD [†] (Li et al. 2023)	65	COCO-sim (Li et al. 2023)	MLG	40.8 4	44.9	30.6	25.0	28.5	16.3	20.7	22.8	15.5	12.9	14.7	8.5
IFSeg (Yun et al. 2023)	80(T)+91(S)	COCO (Mottaghi et al. 2014a)	MC	53.3 5	58.6	40.0	45.6	50.1	34.3	22.6	24.9	17.0	19.5	21.4	14.7
MCLIP* (Zheng Ding 2023)	80(T)+53(S)	COCO (Mottaghi et al. 2014a)	MLG	48.5 5	53.4	36.4	41.5	45.6	31.2	21.6	23.8	16.2	18.7	20.5	14.1
ODISE [†] (Xu et al. 2023)	80(T)+53(S)	COCO (Mottaghi et al. 2014a)	MCG	55.4 6	60.9	41.5	47.4	52.1	35.6	23.1	25.4	17.3	19.9	21.9	15.0
OVSeg* (Liang et al. 2023)	80(T)+91(S)	COCO (Mottaghi et al. 2014a)	MCG	41.7 4	45.9	31.9	35.7	39.6	27.7	21.1	23.2	15.8	18.2	20.0	13.7
OVAM† (Manchón et al. 2024)	×	COCO-cap (Manchón et al. 2024)	MCG	49.2 5	54.1	36.9	19.1	26.3	16.6	22.1	24.3	16.6	13.5	18.0	11.4
SED (Xie et al. 2024)	80(T)+91(S)	COCO (Mottaghi et al. 2014a)	MLG	73.4 8	80.7	55.1	62.7	68.9	47.1	24.1	26.5	18.1	20.8	22.9	15.7
SEEM (Zou et al. 2023)	80	COCO (Mottaghi et al. 2014a)	MLG	69.8	76.8	52.3	39.6	45.5	24.8	23.6	26.0	17.7	17.4	19.4	14.4
		COCO-S (Mottaghi et al. 2014a)													
LISA (Lai et al. 2024)	×	ADE20K (Zhou et al. 2017)	ML	71.5 7	78.0	54.0	51.2	58.3	36.0	24.0	26.4	18.0	19.0	21.0	15.2
		LVIS-PACO (Ramanathan et al. 2023)													
Ours [†]	17	CMHQ (Li et al. 2024)	MCG	85.9 8	88.4	68.8	79.5	82.9	59.3	31.0	34.9	23.8	27.5	30.0	21.7

Table A1: **FPP/CCP evaluation.** The table is divided into two sections: the first covers human parsing and close-set segmentors, while the second includes open-vocabulary segmentors. Both M2F- C_{close} and ODISE- C_{open} are retrained on CosmicManHQ. The best scores are highlighted in **teal**, and the second-best in gray . Each cell reports (mIoU, mAcc, mAP^{SS}@[0.50:0.95]). Diffusion-based methods are denoted by \dagger , and CLIP-based methods by *.

Additional Quantitative Results

Baseline Training Details

In table A1 we summarise baseline models used in Sec. Experiments for human parsing, closed-set, and openvocabulary segmentation. The table lists each model's training categories (Cats.). Parsing models employ fixed label sets with no support for unseen classes, whereas openvocabulary models are typically trained on larger COCO Thing (T) and Stuff (S) sets. GD[†] and OVAM[†] rely on synthetic data; OVAM is trained on only 1,100 COCO-Cap captions, and neither OVAM nor LISA report their training-category counts. Human-parsing baselines were trained on PPP, ATR, CIHP, or LIP; Sapiens was pretrained on Humans-300M and fine-tuned on Humans-2K (H{300M,2K}). We retrain M2F-C_{close} and ODISE-C_{open} on CosmicManHQ (CMHQ). Supervision codes (Supv.): M—GT masks, L—labels, C—captions, G—grounding for predicted masks.

FPP and CCP

In addition to the metrics in Tabs. 1–6 of the main paper, we report FPP and CCP scores for the human-parsing, closed-set, and open-vocabulary baselines in table A1 on Cosmic-ManHQ and GranD-f. Although FPP/CCP masks do not separate body parts or fine-grained clothing—the focus of our work—they provide complementary validation. Each cell lists (mIoU, mAcc, mAPSS@[0.50:0.95]). Because open-vocabulary methods usually evaluate *person* as a single full-body class and many baselines are trained with clothing/accessory labels (e.g., COCO accessories in CCP), we include this comparison. CCP is a subset of COP whose categories are seen during training. As shown, Spectrum surpasses all baselines on every metric; second-best scores are shaded gray. Note that human-parsing models and the retrained closed-set segmentor M2F-C do not output FPP masks, as

they predict only body parts, while PPP-SCHP yields only BHP masks due to its limited label set.

Additional Qualitative Results

Dynamic Mask Color Allocation

As noted in Subsec. Closed-set Segmentors of the main paper, baseline visualisations use their original colour schemes, whereas our method accepts any unseen clothing prompt and dynamically assigns a unique colour to each predicted mask (see fig. A2). In the single and multi-human examples, the colours are selected automatically in our code and shown in the legend at the bottom, while the input caption appears at the top.

Single and Multi-human Results

In figs. A3 and A4 we provide additional qualitative results on the multi-human GranD-f cross-dataset and the single-human CosmicManHQ test set, respectively. Prompts are shown beside the original images. The examples confirm that Spectrum produces accurate, semantically annotated masks for every visible body part and clothing category, including unseen classes, regardless of the number of humans. It also ignores standalone garments and irrelevant objects, as shown in fig. A3 (row 4, col. 1, highlighted in yellow), where a scene with three people and numerous background garments left unsegmented demonstrates the model's robustness.

Challenging Cases

Figure A1 shows challenging cases for Spectrum. Columns 1, 3, and 5 involve heavy occlusion of human parts (column 5 also simulates the low-exposure setting from our ablation); column 2 contains a snow-covered background, and column 4 depicts a densely crowded scene.



Figure A1: **Challenging cases.** Spectrum encounters difficulties in challenging scenarios involving heavy occlusion, low exposure, complex compositions (e.g., snow-covered mountain regions), and high crowd density.



Figure A2: **Dynamic mask color assignment.** Assigned colours appear in the legend below, and the input prompt is shown above.

Prompt Inputs and Ensembling

During inference, the model takes an image x and a natural-language description in one of several forms—openvocabulary labels (e.g., sarees, military uniform), a caption (e.g., "Man in military dress and boots holding a handbag, walking with a baby in a dress"), or ensemble labels (Ghiasi et al. 2022a) (e.g., jumpsuit, wedding dress as novel terms under one-piece outfit)—together with Extended Body Part (EBP) labels to handle prompts that omit body parts. Ensemble labels comprise lists of sub-categories, synonyms, and plurals of the original training classes. We provide ensembling examples for CosmicMan-HQ mask categories, including bottom, one-piece outfit, hat, and special clothing.

- bottom → pants, trousers, jeans, shorts, sweatpants, bikini bottom, skirt, leggings, cargo pants, mini, short, knee-high, high-low, straight, flare, close-fitting, tapered, wide-leg
- one-piece outfit → dress, dresses, one-piece swimsuit, bathrobe, romper, bodysuit, wedding dress, jumpsuit
- hat \rightarrow cap, caps, beret, sun hat, beanie hat, bucket hat,

helmet, baseball cap, cowboy hat

 special clothing → costume, costumes, hanfu, taekwondo uniform, graduation gown, kimono, police uniform, cheongsam, cosplay, traditional costumes, fire suit, hazmat suit, judicial robe

\mathcal{L}_{BCE} and \mathcal{L}_{DICE} Losses

As part of our full loss (Eq. (5)), we define the standard \mathcal{L}_{BCE} and \mathcal{L}_{DICE} losses for class logits and mask supervision respectively:

$$\mathcal{L}_{BCE} = \frac{1}{N} \sum_{i=1}^{N} BCE(\mathbf{p}_{ik}, y_i),$$

$$\mathcal{L}_{DICE} = 1 - \frac{2 \mathbf{y} \cdot \mathbf{p}_k + 1}{\|\mathbf{y}\| + \|\mathbf{p}_k\| + 1}.$$
(A6)

Here, y_i is the ground truth mask category. In $\mathcal{L}_{\text{DICE}}$, the numerator sums the dot product over all pixels $(\sum_{i=1}^N y_i \, \mathbf{p}_{ik})$ while the denominator sums the pixel values for both \mathbf{y} and \mathbf{p}_{ik}^b .

Limitations

Although Spectrum advances detailed diverse clothing and body-part parsing in multi-human scenes, several limitations persist:

Ground-truth masks. Existing datasets (ATR, PPP, LIP, CIHP, CosmicManHQ, GranD-f) offer a baseline, but large-scale collections with consistent high-quality part masks for every person—foreground and background—in real-world scenes are still needed.

Crowded scenes. Spectrum handles multi-person scenes, but very dense crowds remain challenging (fig. A1).

Evolving fashion. Fashion changes rapidly; continual-learning updates will be required to recognise new and shifting clothing styles.

Ethical Considerations

We build on publicly available models—Stable Diffusion, OpenCLIP, TexDreamer, BERT NER, and CLIP variants—and datasets (CosmicManHQ, GranD-f, ATLAS, ATR, LIP, PPP, CIHP, LAION). While our method is not inherently designed for discriminatory or inappropriate use, any biases present in these public resources can propagate to our trained model.



Figure A3: **Additional qualitative results on GranD-f.** In Row 2, Col. 1, Spectrum ignores background garments in a cluttered three-person scene (one person partly occluded) and cleanly parses only the relevant body parts and diverse clothing, demonstrating its robustness.

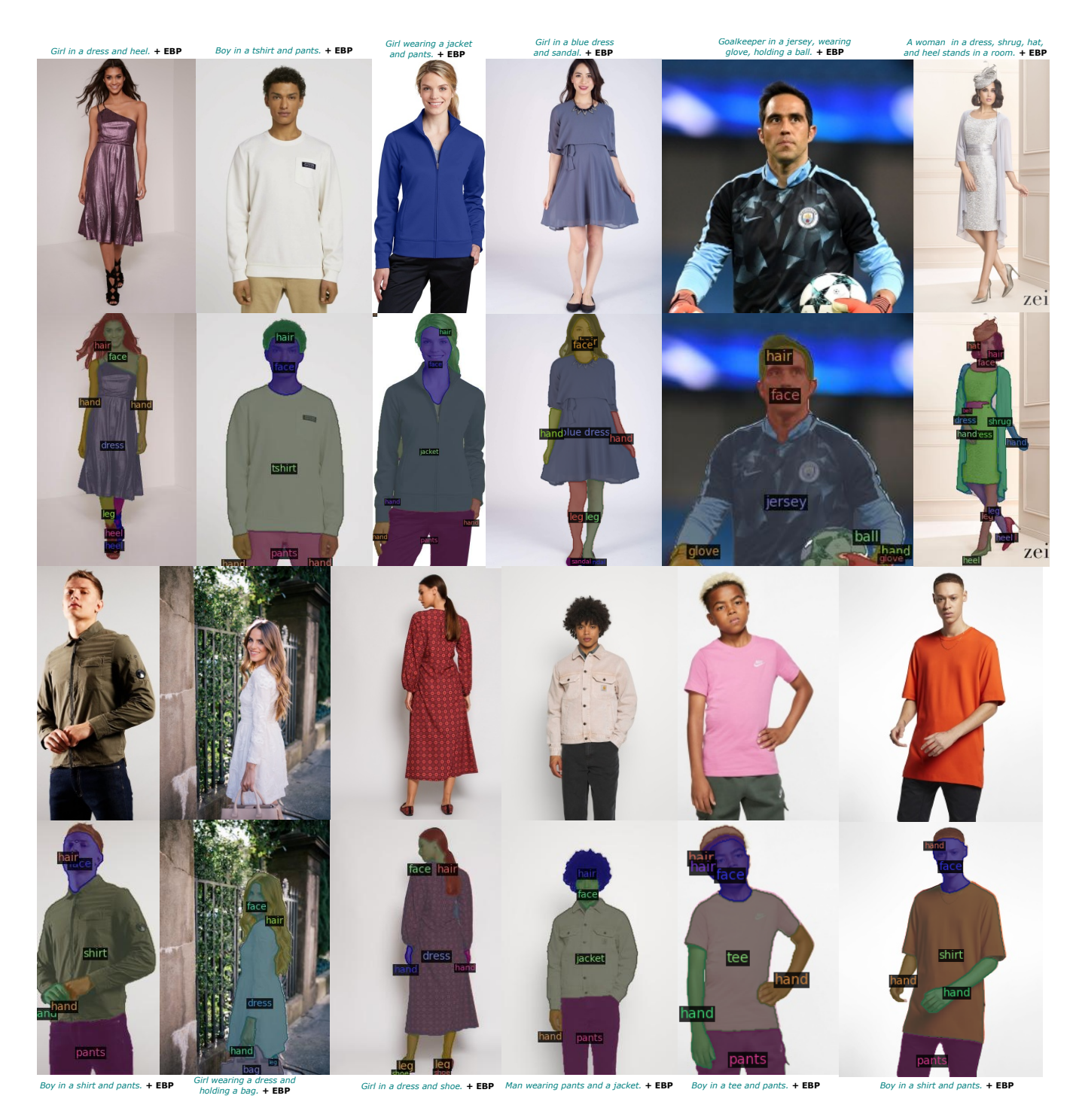


Figure A4: Additional qualitative results on the CosmicManHQ test set.